FTIR Study of N_2O_3 on Porous Glass at Room Temperature

Michihiro Mochida† and Barbara J. Finlayson-Pitts*

Department of Chemistry, University of California, Irvine, Irvine, California 92697-2025

Received: April 18, 2000; In Final Form: June 27, 2000

While N_2O_3 has been observed previously in the gas phase, in solution and as a solid at low temperatures, it has not been reported adsorbed on solids at room temperature. However, the adsorbed species has been postulated as a precursor to HONO in the lower atmosphere. We report here the formation of N_2O_3 adsorbed on a porous glass surface at room temperature from the precursors NO and NO_2 using transmission FTIR spectroscopy. The spectrum of the porous glass in the presence of NO and NO_2 showed broad peaks at approximately 1870 and 1600 cm^{-1} attributed to surface adsorbed *asym*-N_2O_3 ($ONNO_2$). These peaks shifted by ∼30−40 cm^{-1} to lower wavenumbers when ^{15}N-labeled NO was used, consistent with absorption bands previously assigned by other researchers to solid *asym*-N_2O_3 at low temperature. While the peaks assigned to surface-adsorbed *asym*-N_2O_3 did not decrease significantly on exposure to water vapor, measurable concentrations of gas-phase HONO were formed. The atmospheric implications are discussed.

Introduction

Dinitrogen trioxide (N_2O_3) exists in the gas, aqueous, and solid phases, and is commonly observed as a blue solid when NO and NO_2 are co-condensed.[1] It is formed in an equilibrium reaction between NO and NO_2:[2,3]

$$NO + NO_2 + M \leftrightarrow N_2O_3 + M \quad K_1 = 0.59\ atm^{-1} \quad (1, -1)$$

and has been characterized in a number of experimental and theoretical studies.[4−20]

There are two isomeric forms of N_2O_3, the asymmetric $ONNO_2$ and the symmetric ONONO,[6−8,12−14,17,20−22] and for each of these exist different conformers.[20] Infrared spectra of *asym*-N_2O_3 and *sym*-N_2O_3 have been reported in low-temperature matrixes [7,12,21,22] and in liquid xenon.[13] Most theoretical and experimental studies report that *sym*-N_2O_3 is less stable than *asym*-N_2O_3 by amounts estimated between 1.4 and 9.4 kcal mol^{-1}.[7,13,17,20,23] Holland and Maier reported that with an energy difference of 1.8 ± 0.2 kcal mol^{-1}, the *sym*-N_2O_3 in gas phase is about 4% of total N_2O_3 at 300 K.[13] If we extrapolate these results to a difference of 9.4 kcal mol^{-1},[17] only 1×10^{-5}% of the total N_2O_3 would be present in the symmetric form at room temperature. Thus, the asymmetric form is the isomer commonly observed in the gas phase by infrared spectroscopy.[4,8,24]

N_2O_3 has been suggested as an intermediate in the formation of nitrous acid in the reaction of NO, NO_2 and water:

$$NO + NO_2 + H_2O \leftrightarrow 2HONO \quad (2, -2)$$

In the lower atmosphere, particularly in urban areas, HONO is a major source of the hydroxyl radical (OH), which initiates the oxidation of organics in air.[25] However, its sources are not well understood, although from laboratory studies, heterogeneous reactions appear to be important. For example, the heterogeneous hydrolysis[26] of NO_2,

$$2\ NO_2 + H_2O \leftrightarrow HONO + HNO_3 \quad (3, -3)$$

(or an N_2O_4 intermediate)[27,28] is believed to be a key HONO source in the atmosphere. On the other hand, some field studies reported correlations between atmospheric concentrations of HONO with not only NO_2, relative humidity, and particles in air, but also with NO.[29−31] A potential reason for the dependence on NO is the formation of N_2O_3 as shown in reaction 1, followed by the heterogeneous reaction of N_2O_3 with water, i.e. overall reaction 2. Reaction 2 is known to be too slow in the gas phase to be responsible for this correlation,[32] but the kinetics are enhanced in the presence of surfaces.[33−39] However, while N_2O_3 has been identified on gold surfaces with or without co-condensed water,[40−42] in low-temperature matrixes, [5,7,12,15,16,18,21,22] in liquid xenon,[13] and in the gas phase,[4,8,24] it has not, to our knowledge, been reported on surfaces at room temperature. We report here the results of FTIR studies in which N_2O_3 adsorbed on porous glass (a silica surface) has been identified at room temperature from the reaction of NO and NO_2. The atmospheric implications are discussed.

Experimental Section

The apparatus, described in detail elsewhere,[28] consists of a cylindrical borosilicate glass cell mounted in the sampling compartment of an FTIR spectrometer (Research Series, Mattson). The cell had a path length of 6.7 cm, volume of 79 cm^3, and geometric surface area estimated to be 240 cm^2. A porous glass plate suspended in the cell could be moved in and out of the infrared beam. Single beam spectra were recorded with the porous glass either in the path of the infrared beam or withdrawn from the beam, as well as with and without the gases in the cell. The ratio of the single beam spectrum with the porous glass and gases in the beam to that without the reactants allows the silica absorptions to be ratioed out, giving the absorbance due to gases plus surface-adsorbed species. Similarly, the ratio of the analogous single beam spectra with and without the gases and with the porous glass withdrawn from the infrared beam was used to obtain the absorbance of the gases alone. Subtracting the spectrum of the gas species from that of the combined gas

* To whom correspondence should be addressed. Phone: (949) 824−7670. Fax: (949) 824−3168. E-mail bjfinlay@uci.edu.

† Current address: Institute of Low Temperature Science, Hokkaido University, N19 W8, Kita-ku, Sapporo 060-0819, Japan.

10.1021/jp001484o CCC: $19.00
Published on Web 08/09/2000

plus surface species gives the spectrum due to surface-adsorbed species alone. Infrared spectra were recorded with resolution between 0.5 and 4 cm^{-1} and the number of scans was between 1 and 1024, depending on the S/N ratio and time resolution required for experiments.

Since porous glass has a strong absorbance[43] below 2000 cm^{-1} where vibrational bands of nitrogen oxides are present, the porous glass plate must be as thin as possible in order to obtain sufficient intensity of the transmitted infrared beam. A commercially available (Corning) 2 × 3 cm porous glass plate of 1 mm thickness was etched in the center with 7.7(v:v)% HF solution for 21 min to obtain a plate with an ~3 cm^2 central area as thin as 0.1 mm which was investigated by the infrared beam. The porous glass plate has a surface area of 28.5 ± 0.3 m^2 as determined by the Brunauer−Emmett−Teller (BET) method using nitrogen as an adsorbate (ASAP2000, Micromeritics); this large surface area, relative to the geometric area of the plate of 12 cm^2, is due to the numerous small pores in the glass.[44] However, as discussed in more detail below, the experimental evidence suggests that not all of this surface area is available for uptake of gases, perhaps because of water in the pores under our experimental conditions, and/or the larger size of N_2O_3 compared to N_2 used for the BET measurements.

Between experiments, the porous glass was cleaned by soaking in water (Barnstead, Nanopure, 18 MΩ cm) to remove adsorbed species such as nitrate and nitrite. It was then pumped for ~2 h prior to exposure to the gases. In agreement with previous work,[43] this procedure does not remove water strongly bound to the surface as indicated by a broad infrared absorption in the 3400 cm^{-1} region. In most experiments, there was no heating of the surface before reaction, because the intent was to study the reactions on a hydrated surface. In one set of experiments to elucidate the effects of water vapor on the surface species, the porous glass was heated at 520 K for several hours under vacuum and then cooled to room temperature prior to addition of the gases and water vapor.

Both NO and NO_2 were measured by FTIR using the bands centered at 1876 and 1618 cm^{-1}, respectively. Quantification was carried out using calibrations for these gases under the conditions of temperature and pressure used in these experiments. Gas-phase N_2O_3 was quantified using the integrated band intensity at 1830 cm^{-1} of (660 ± 111) cm^{-2} atm^{-1} reported by Kagann and Maki.[24] It was assumed that the absorbance was linear with concentration over the range measured in these experiments.

Nitric oxide (Matheson 99%) was passed through a dry ice/acetone bath at 195 K to remove impurities such as NO_2 and HNO_3. Nitrogen dioxide was synthesized by combining NO with excess oxygen (Oxygen Service Company, 99.993%) and then was purified by condensing the mixture at 195 K using a dry ice/acetone bath and pumping away the excess O_2. NO_2 was stored in a glass bulb covered with a dark cloth to minimize photolysis in room lights.

Results and Discussion

A. Evidence for N_2O_3 Adsorbed on Porous Glass. Figure 1 shows infrared spectra when a set amount of NO_2 and increasing amounts of NO were added to the cell with the suspended porous glass plate. These spectra include both the gas phase and species adsorbed on the porous glass. As expected, the gas-phase NO_2 and NO bands centered at 1618 and 1876 cm^{-1}, respectively, are clearly visible. The band at 1740 cm^{-1} is due to N_2O_4 (both gas phase and adsorbed) which is in equilibrium with NO_2. When NO_2 was introduced into the cell alone, a broad band at ~1677 cm^{-1}, assigned to nitric acid adsorbed on the porous glass,[27,28,45] was observed. The nitric acid is mainly due to hydrolysis of the NO_2 on the hydrated silica surface,[28] perhaps with some contribution from small amounts of impurity HNO_3 in the NO_2. The surface-adsorbed HNO_3 decreases upon the addition of NO, due to the rapid reaction of the surface species with NO to form NO_2.[45] In addition, a broad peak can be seen growing under the P branch of the NO rotational bands.

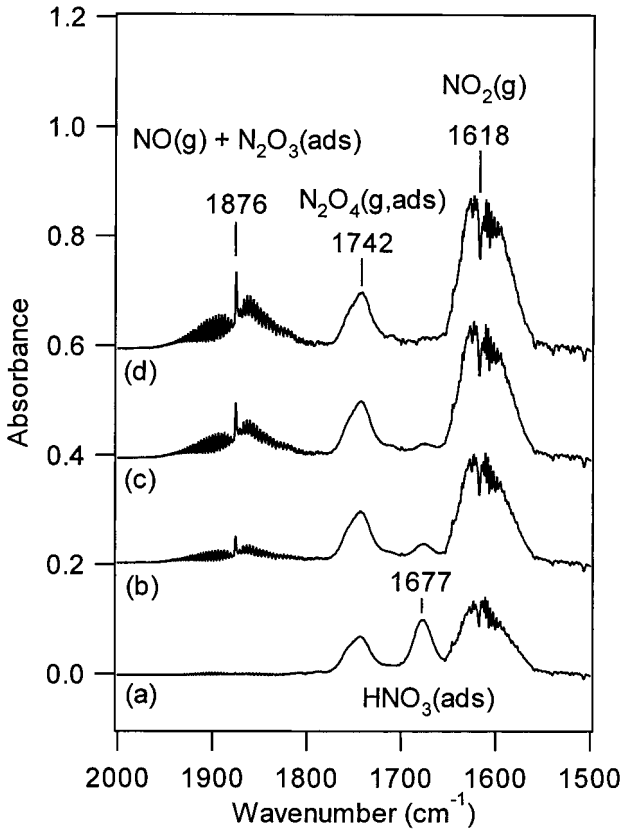

Figure 1. Infrared spectra of combined gas and adsorbed species after the introduction of (a) NO_2/N_2O_4 (1.7×10^{17} molecule cm^{-3}) into the reaction cell containing the porous glass followed by NO at concentrations of (b) 3.0×10^{17}, (c) 6.4×10^{17}, and (d) 9.5×10^{17} molecule cm^{-3}, respectively.

Figure 2a shows the combined spectrum of gases and surface-adsorbed species in the 1500−2000 cm^{-1} region for a typical experiment. Figure 2b is the spectrum of the gas phase only, obtained by lifting the porous glass sample out of the infrared beam. By subtracting from Figure 2b the contributions of NO, NO_2, and N_2O_4, a weak band centered at 1830 cm^{-1} is observed, as shown in Figure 2c. This band compares well with the ν_1 stretch of N_2O_3 in the gas phase.[4,8,24] Using $K_1 = 0.59$ atm^{-1} and correcting the NO_2 concentration for the equilibrium amount of N_2O_4, the gas-phase N_2O_3 concentration is calculated to be 7×10^{15} molecule cm^{-3}. This is in reasonable agreement with a concentration of 5×10^{15} molecule cm^{-3} calculated using the integrated band intensity reported by Kagann and Maki,[24] particularly given the relatively small amounts of N_2O_3 and the need to ratio out or subtract the contributions of the porous glass and other gases present in the cell. Another N_2O_3 peak around 1650 cm^{-1} was not clearly discernible due to the difficulty in subtracting the strong NO_2 absorption. The integrated band intensities for gas-phase NO_2[46] and N_2O_3[24] are similar, (636 ± 25) cm^{-2} atm^{-1} and (660 ± 111) cm^{-2} atm^{-1}, respectively (both base 10). The much larger gas-phase NO_2 infrared band

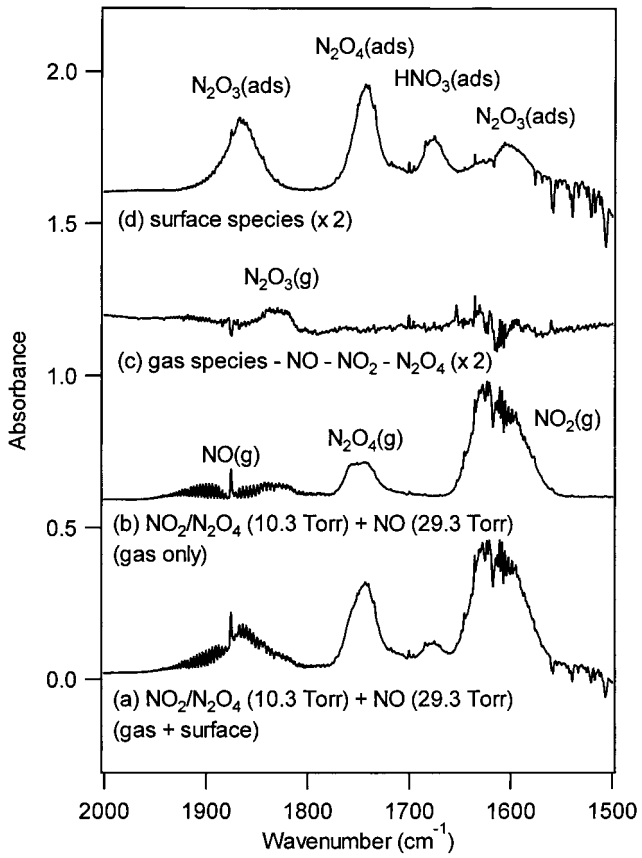

Figure 2. Infrared spectra of (a) gas and surface species after the introduction of 3.3×10^{17} molecule cm^{-3} of NO_2/N_2O_4 and 9.5×10^{17} molecule cm^{-3} of NO into the cell containing the porous glass; (b) gas phase under the same conditions as for (a); (c) difference spectrum obtained by subtraction of NO(g), NO_2(g), and N_2O_4(g) bands from (b); (d) difference spectrum between (a) and (b), showing only surface-adsorbed species. The total intensities in parts (c) and (d) have been multiplied by two for clarity.

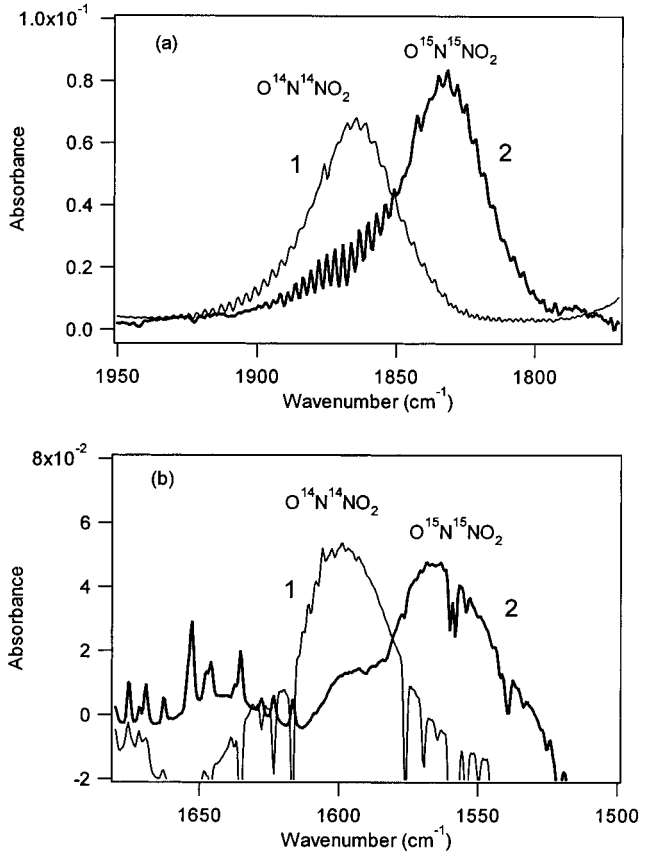

Figure 3. Infrared bands of surface-adsorbed N_2O_3 with two isotopes: ^{14}N and ^{15}N. (a) with (1) ^{14}NO (9.7×10^{17} molecule cm^{-3}) and $^{14}NO_2$ (1.6×10^{17} molecule cm^{-3}) or (2) ^{15}NO (1.1×10^{18} molecule cm^{-3}) and $^{15}NO_2$(1.7×10^{17} molecule cm^{-3}) in the cell; (b) with (1) ^{14}NO (1.1×10^{18} molecule cm^{-3}) and $^{14}NO_2$ (2.4×10^{17} molecule cm^{-3}) or (2) ^{15}NO (1.1×10^{18} molecule cm^{-3}) and $^{15}NO_2$ (1.7×10^{17} molecule cm^{-3}) in the reaction cell. The concentrations for NO_2 given are total NO_2 and the N_2O_4 in equilibrium with it.

compared to that for N_2O_3 (Figure 2) is consistent with its much higher concentration, 3×10^{17} vs $(5-7) \times 10^{15}$ molecule cm^{-3} for N_2O_3.

Figure 2d shows the spectrum of the surface-adsorbed species, obtained by subtracting the gas spectrum in Figure 2b from the combined "gas + surface-adsorbed" spectrum in Figure 2a. In addition to N_2O_4 and HNO_3 on the surface, two broad peaks at ~1870 and ~1600 cm^{-1} were observed. As expected for surface species, rotational structure is not evident. The peaks at ~1870 and 1600 cm^{-1} correspond to those reported for solid *asym*-N_2O_3 at low temperatures,[5,7,21,22,40,41] and hence we assign them to the nitrosyl NO stretch (1870 cm^{-1}) and the nitro−NO stretch (~1600 cm^{-1}) of *asym*-N_2O_3 adsorbed on the porous glass. These absorption peaks were observed only when both NO and NO_2 were present. No surface absorptions due to NO or NO_2, respectively, were observed when these gases were introduced individually into the cell (although as reported in earlier studies,[28] N_2O_4 and HNO_3 are formed on the surface from NO_2). Hence, attribution of these bands to species such as the *cis*-N_2O_2 dimer of NO observed on zeolites[47,48] or to NO_2 strongly bonded to the surface with the partial loss of an electron[48] can be ruled out. In contrast to the gas-phase absorption spectrum, the peak due to adsorbed N_2O_3 on the surface is larger than that of NO_2. Thus, the amount of N_2O_3 on silica surfaces is apparently enhanced compared to that of NO_2, as was observed for NO_2/N_2O_4 on silica surfaces.[28]

Additional evidence for assignment of the 1870 and 1600 cm^{-1} peaks to surface-adsorbed N_2O_3 was obtained using ^{15}N-labeled NO and NO_2. As seen in Figure 3a, both of these peaks shifted to lower wavenumbers by approximately 30−40 cm^{-1}. Similar shifts have been observed for solid N_2O_3 at low temperatures where the 1870 cm^{-1} band shifted by ~32 cm^{-1} from the ^{14}N to the ^{15}N compound, while the second band shifted to lower wavenumbers by ~40 cm^{-1}.[12,22]

In short, both the peak positions and their shifts when ^{15}N is used support the assignment of the peak at 1830 cm^{-1} to the nitrosyl-NO stretching mode of *asym*-N_2O_3, and that around 1600 cm^{-1} to the nitro-NO stretching mode of *asym*-N_2O_3.[12,22]

B. Dependence of Gas and Surface-Adsorbed N_2O_3 on Gas-Phase NO and NO_2. Figure 4a shows the concentration of gas-phase N_2O_3, calculated using the integrated band intensity for the υ_1 stretch at 1830 cm^{-1} reported by Kagann and Maki[24] as a function of the initial NO concentration at two different initial concentrations of NO_2. As expected from the equilibrium (eq 1, −1), the gas phase intensity increases linearly with the NO concentration; the concentrations determined from the infrared band intensities are consistent within experimental error with those calculated using the equilibrium constant and the initial concentrations of NO and NO_2. (The small slope when NO_2 was not added and small nonzero intercepts are due to the difficulty in obtaining complete subtraction of the strong porous glass and gas-phase NO absorptions in this region; in addition, some NO_2 is formed in the cell when NO is added, due to its reaction with small amounts of HNO_3 left adsorbed on the

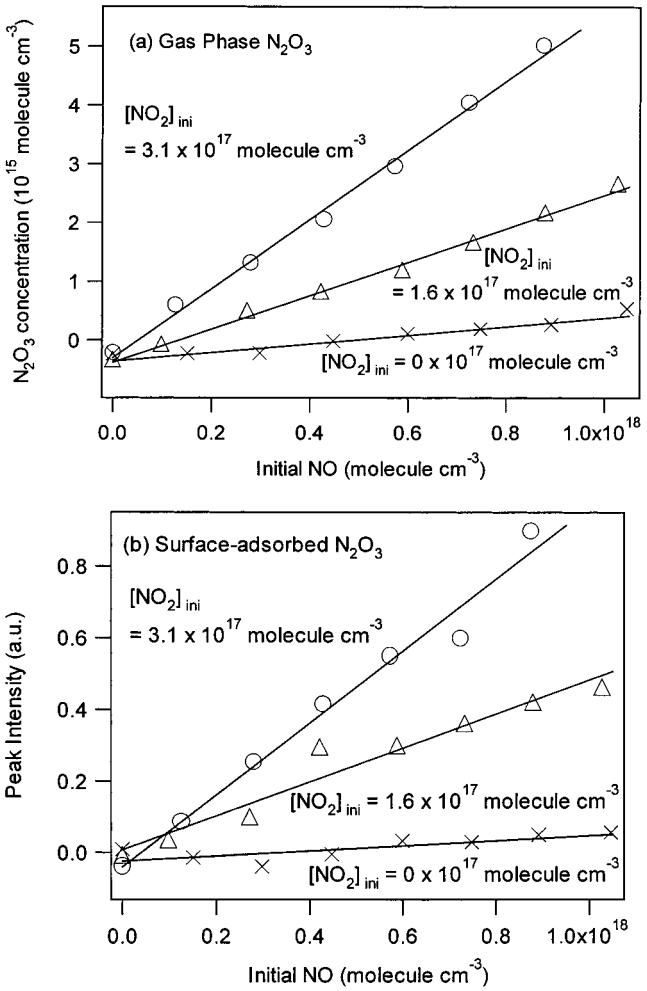

Figure 4. Measured (a) gas-phase concentrations of N_2O_3 measured using the 1830 cm^{-1} band, and (b) integrated intensities of the band at 1870 cm^{-1} due to surface-adsorbed N_2O_3 when increasing amounts of NO are added to an initial NO_2/N_2O_4 mixture at the initial concentrations of NO_2 shown which have been corrected for the $2NO_2 \leftrightarrows N_2O_4$ equilibrium.

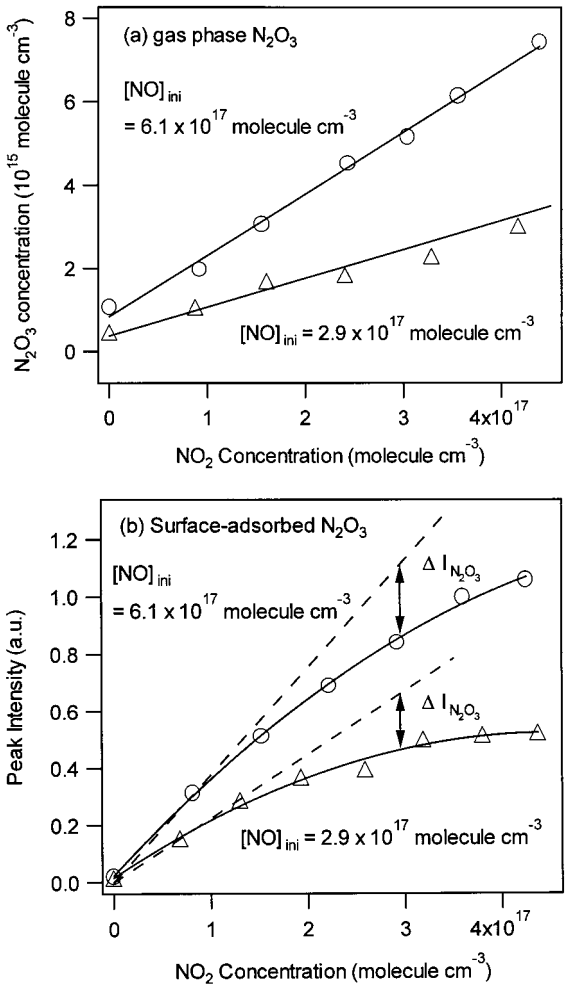

Figure 5. Measured (a) gas-phase concentrations of N_2O_3 using the 1830 cm^{-1} band, and (b) integrated intensities of the band at 1870 cm^{-1} due to surface-adsorbed N_2O_3 when increasing concentrations of NO_2/N_2O_4 are added to either (2.9 or 6.1) $\times$ 10^{17} molecule cm^{-3} NO in the cell. The concentrations of NO_2 have been corrected for the $2NO_2 \leftrightarrows N_2O_4$ equilibrium.

surface [45] from previous runs). Figure 4b shows that the intensity of the peak at 1870 cm^{-1} assigned to surface-adsorbed N_2O_3 also increases linearly with NO. (The band at 1600 cm^{-1} was too weak to provide a meaningful correlation with the gas-phase species).

Figure 5 shows the analogous plots for N_2O_3 as a function of the initial gas-phase NO_2 concentration, which was calculated from the total pressure of NO_2/N_2O_4 and the equilibrium constant for the $2NO_2 \leftrightarrow N_2O_4$ reaction, $K_{eq} = 2.5 \times 10^{-19}$ cm^3 $molecule^{-1}$.[49] While the gas-phase N_2O_3 varies linearly with NO_2, the peak intensity at 1870 cm^{-1} for the adsorbed species falls off at higher NO_2 concentrations. Given that N_2O_4 is enhanced on the surface relative to the gas phase,[28] a possible explanation is that N_2O_4 competes with N_2O_3 for the surface sites at the higher concentrations, leading to the observed falloff in the surface N_2O_3. If this is the case, then the difference between the expected ideal linear behavior shown by the dotted lines and the observed peak intensities, represented as $\Delta I_{N_2O_3}$ in Figure 5b, should be proportional to the amount of surface N_2O_4 and hence to gas-phase N_2O_4 or $[NO_2]^2$. Figure 6 shows a plot of this difference, $\Delta I_{N_2O_3}$, as a function of the square of the NO_2 pressure for the two different concentrations of NO. The linearity of these plots shows that competition for surface sites between N_2O_4 and N_2O_3 is indeed responsible for the nonlinear dependence of surface-adsorbed N_2O_3 on the gas-phase NO_2 concentration seen in Figure 5b.

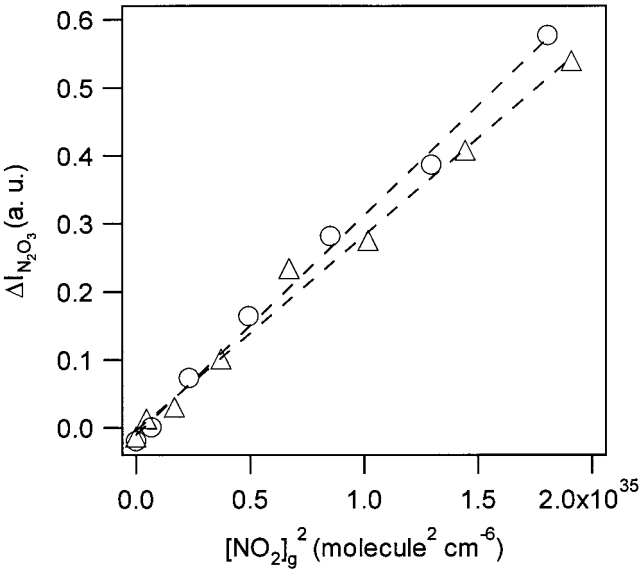

Figure 6. The difference ($\Delta I_{N_2O_3}$) shown in Figure 5 as a function of square of the NO_2(g) concentration. Circles and triangles are plots at NO concentrations of 2.9 and 6.1 $\times$ 10^{17} molecule cm^{-3}, respectively.

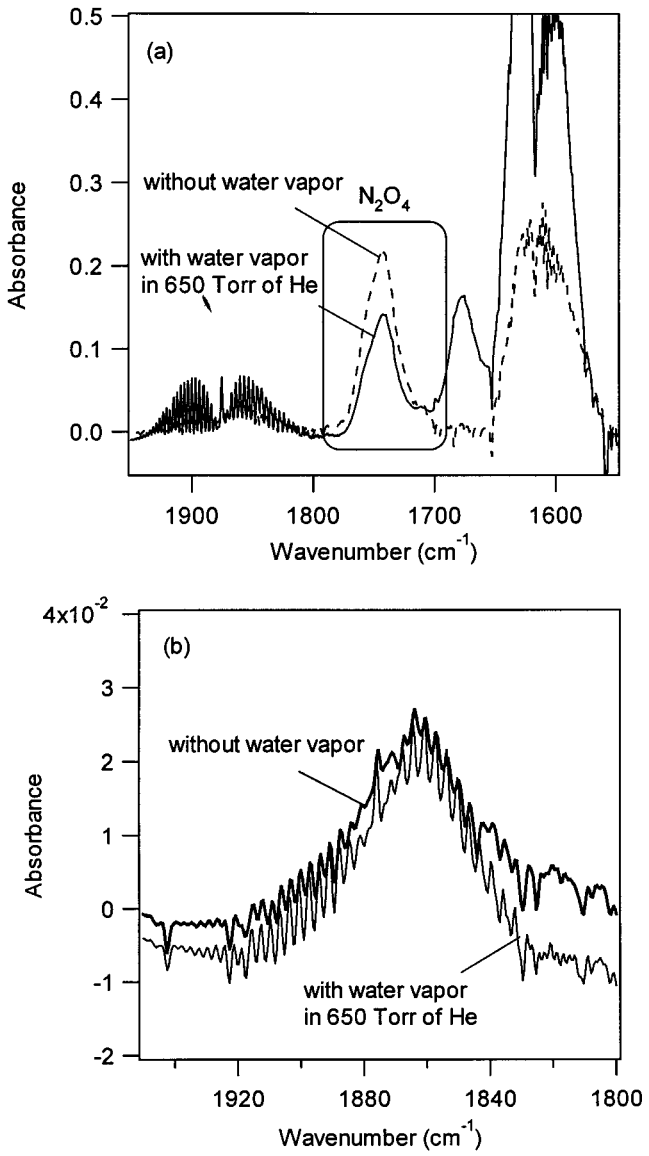

Figure 7. Infrared spectra of (a) the gas-phase plus surface-adsorbed species before adding water (dashed line) and after adding water vapor, and (b) spectrum of surface-adsorbed N_2O_3 before and after the addition of water vapor. The initial concentration of NO was 3.0×10^{17} molecule cm^{-3} and NO_2 was 2.5×10^{17} molecule cm^{-3}. The water vapor concentration added to the cell in 650 Torr of He was 6.6×10^{17} molecule cm^{-3}. The cell with the porous glass had been heated to 520 K for several hours prior to introducing the gases.

C. Effects of Added Water Vapor. Reaction 2 may involve adsorbed N_2O_3 as an intermediate which then reacts with water on the surface. N_2O_3 is the anhydride of HONO, and is known to react in aqueous solution with H_2O to form HONO:[50]

$$N_2O_3 + H_2O \leftrightarrow 2HONO \qquad (4, -4)$$

To test whether surface-adsorbed N_2O_3 reacts with water vapor, the porous glass was first heated to 520 K for several hours under vacuum; this decreased the peak height due to water at 3400 cm^{-1} by a factor of approximately 2−3. N_2O_3 was generated on the surface in the usual manner and water vapor was then added to the cell. The dashed line in Figure 7a shows the initial spectrum of the gas and surface species. The solid line shows the spectrum after water vapor in 650 Torr He was added to the cell. The N_2O_4 peak decreased and that of adsorbed HNO_3 increased, as expected from previous studies in this

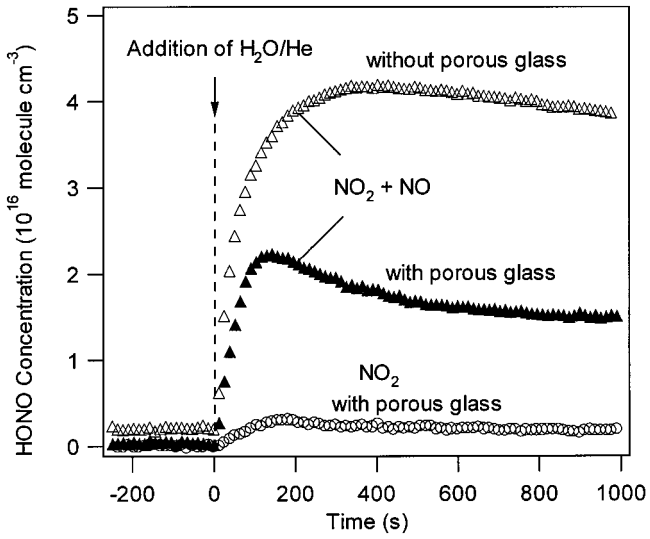

Figure 8. Time−concentration profiles of HONO with 1.1×10^{18} molecule cm^{-3} of NO and 1.6×10^{17} molecule cm^{-3} of NO_2 in the cell before and after the addition of 6.6×10^{17} molecule cm^{-3} of water vapor in 650 Torr of He. ▲ represents HONO with the porous glass suspended in the cell; the cell with the porous glass had been heated to 520 K for several hours prior to introducing the gases. Δ represent HONO without the porous glass in the cell. Smaller amounts of HONO generated with only NO_2 in the cell with the porous glass are represented by O.

laboratory.[28] (The apparent increase in the NO and NO_2 is due to pressure effects on the bands). However, as seen in Figure 7b, the 1870 cm^{-1} N_2O_3 peak did not change significantly upon the addition of water vapor.

The formation of gas-phase HONO was followed with time under the experimental conditions similar to the ones shown in Figure 7. Despite the lack of change in surface-adsorbed N_2O_3, gas-phase HONO was formed (Figure 8). However, the amount of HONO formed without the porous glass plate in the cell was about twice that when the porous glass plate was present. This initially puzzling result may be due to the fact that the effective surface area for the reaction on the porous glass plate is much closer to its geometric surface area than to the measured BET surface area. In that case, most of the heterogeneous chemistry is actually occurring on the walls of the reaction cell, rather than on the porous glass plate. Following the surface species on the porous glass plate using FTIR provides a means of directly following the chemistry occurring on all of the cell surfaces. The smaller amount of HONO formed in the presence of the porous glass may be due to two factors: (1) a heterogeneous loss of HONO by reaction with HNO_3 on the porous glass plate suggested by studies of the reaction of surface-adsorbed HNO_3 with NO in this system,[45] and/or (2) efficient uptake of water vapor by the porous glass so that the surfaces of the reaction cell are actually drier when it is suspended in the cell.

The lack of change in the surface-adsorbed N_2O_3 when water vapor is added may be attributed to one or more factors. One possibility is that the amount of N_2O_3 lost from the surface by hydrolysis is too small to be observed. We estimate that the loss would have to be ≥20% in order to be readily observed in these experiments. Another possibility is that the symmetrical form of N_2O_3, i.e., ONONO, reacts more rapidly with water than the asymmetrical form, $ONNO_2$, to form HONO. This is reasonable since the reaction of H_2O with *sym*-N_2O_3 presumably occurs with a more-favored six-membered transition state compared to a five-membered transition state for *asym*-N_2O_3.

A small amount of *sym*-N_2O_3 adsorbed on the surface would not be detectable in these experiments, particularly given the overlap of its absorption bands with other species such as HNO_3 and N_2O_4 in our system.[12,20] A third possibility is that surface-N_2O_3 is replenished rapidly from gas-phase NO and NO_2 as it reacts with water.

Finally, it may be that N_2O_3 is not an intermediate in HONO formation, i.e. the reaction of NO and NO_2 at the surface, and not N_2O_3, leads to HONO formation. This could, in principle, occur as a single step or through a sequence of reactions. For example, gas-phase NO_2 is known to react with surface-adsorbed water on the porous glass, forming HNO_3 on the surface.[28] This HNO_3 can react with NO rapidly, likely forming HONO and NO_2.[45]

$$2NO_2(g) + H_2O \xrightarrow{\text{surface}} HONO(g) + HNO_3(ads) \quad (5)$$

$$NO(g) + HNO_3(ads) \xrightarrow{\text{surface}} HONO(g) + NO_2(ads) \quad (6)$$

$$\text{Net Reaction: } NO(g) + NO_2(g) + H_2O \xrightarrow{\text{surface}} 2HONO(g) \quad (7)$$

In short, the mechanism of the observed formation of HONO from the heterogeneous reaction of NO, NO_2, and water and whether it involves N_2O_3 as an intermediate on the surface is not clear.

D. Atmospheric Implications. Regardless of the detailed mechanism of HONO formation from NO, NO_2, and water, this reaction appears unlikely to be important under atmospheric conditions. Assume relatively high concentrations of 100 ppbv each of NO and NO_2 and a particle concentration of 10^4 cm^{-3} with 1 μm radius. Taking the initial rate of HONO formation in Figure 8 and scaling linearly for the NO and NO_2 concentrations and the lower limit of surface areas available for reaction, which is approximately 240 cm^2, the formation of only 2×10^3 molecule cm^{-3} of HONO, i.e. $\sim 1 \times 10^{-7}$ ppbv, are expected after 8 h if there is no simultaneous loss due to deposition, reactions, etc. This is many orders of magnitude smaller than typical concentrations of 1−10 ppbv observed under polluted conditions.[25,26] In short, the heterogeneous reaction of NO and NO_2 with water seems unlikely to be responsible for the correlation of HONO with NO observed in some field studies.[29−31]

Conclusions

Broad infrared absorption bands around 1870 and 1600 cm^{-1} due to adsorbed species on the surface of porous glass were observed in the presence of NO and NO_2 at room temperature. By comparison to literature reports of N_2O_3 at low temperatures and in matrixes, these are assigned to *asym*-N_2O_3, which has not previously been reported on surfaces at room temperature. This assignment has been confirmed using isotopically labeled ^{15}NO which shifts both peaks to lower wavenumbers as expected. The peak intensity of this adsorbed N_2O_3 is proportional to the gas-phase NO concentration, whereas a saturation effect was observed when a large amount of NO_2 was present due to competition for surface sites between N_2O_4 and N_2O_3. The peak at 1870 cm^{-1} due to the *asym*-N_2O_3 did not decrease upon exposure to water vapor, although the formation of gas-phase HONO was observed, which may be due to a number of different factors. Extrapolation of the measured rate of HONO formation to atmospheric conditions suggests that the heterogeneous reaction of NO, NO_2, and H_2O is unlikely to be a significant source of HONO in the atmosphere, in agreement with the results of previous laboratory studies.

Acknowledgment. The authors are grateful to the California Air Resources Board (Contract No. 97-311) and Research Fellowships of the Japan Society for the Promotion of Science for Young Scientists for support of this work. We also thank J. N. Pitts., Jr., for helpful discussions, B. E. Koel for providing preprints prior to publication, and T. J. Wallington for comments on the manuscript..

References and Notes

(1) Beattie, I. R. *Prog. Inorg. Chem.* **1963**, *5*, 1−26.
(2) Smith, I. W. M.; Yarwood, G. *Chem. Phys. Lett.* **1986**, *130*, 24−28.
(3) Markwalder, B.; van den Bergh, H. *J. Phys. Chem.* **1993**, *97*, 5260−5265.
(4) D'Or, L.; Tarte, P. *Bull. Soc. R. Sci. Liege* **1953**, *22*, 276.
(5) Snyder, R. G.; Hisatsune, I. C. *J. Mol. Spectrosc.* **1955**, *1*, 139.
(6) Devlin, J. P.; Hisatsune, I. C. *Spectrochim. Acta* **1961**, *17*, 218−225.
(7) Varetti, E. L.; Pimentel, G. C. *J. Chem. Phys.* **1971**, *55*, 3813−3821.
(8) Bibart, C. H.; Ewing, G. E. *J. Chem. Phys.* **1974**, *61*, 1293−1299.
(9) Bradley, G. M.; Siddall, W.; Strauss, H. L.; Varetti, E. L. *J. Phys. Chem.* **1975**, *79*, 1949−1953.
(10) Stockwell, W. R.; Calvert, J. G. *J. Photochem.* **1978**, *8*, 193−203.
(11) Kishner, S.; Whitehead, M. A.; Gophinathan, M. S. *J. Am. Chem. Soc.* **1978**.
(12) Nour, E. M.; Chen, L.-H.; Laane, J. *J. Phys. Chem.* **1983**, *87*, 1113−1120.
(13) Holland, R. F.; Maier, W. B., II. *J. Chem. Phys.* **1983**, *78*, 2928−2941.
(14) Jubert, A. H.; Varetti, E. L.; Villar, H. O.; Castro, E. A. *Theor. Chim. Acta* **1984**, *64*, 313−316.
(15) Chewter, L. A.; Smith, I. W. M.; Yarwood, G. *Mol. Phys.* **1988**, *63*, 843−864.
(16) Simon, A.; Horakh, J.; Obermeyer, A.; Borrmann, H. *Angew. Chem., Int. Ed. Engl.* **1992**, *31*, 301−303.
(17) Vladimiroff. *J. Mol. Struct.* **1995**, *342*, 103−108.
(18) Horakh, J.; Borrmann, H.; Simon, A. *Chem. Eur. J.* **1995**, *1*, 389−393.
(19) Georges, R.; Liévin, J.; Herman, M.; Perrin, A. *Chem. Phys. Lett.* **1996**, *256*, 675−678.
(20) Wang, X.; Zheng, Q.; Fan, K. *J. Mol. Struct.* **1997**, *403*, 245−251.
(21) Fateley, W. G.; Bent, H. A.; Crawford, B., Jr. *J. Chem. Phys.* **1959**, *31*, 204−217.
(22) Hisatsune, I. C.; Devlin, J. P.; Wada, Y. *J. Chem. Phys.* **1960**, *33*, 714−719.
(23) Stirling, A.; Papai, I.; Mink, J.; Salahub, D. R. *J. Chem. Phys.* **1994**, *100*, 2910.
(24) Kagann, R. H.; Maki, A. G. *J. Quant. Spectrosc. Radiat. Transfer* **1984**, *31*, 173−176.
(25) Winer, A. M.; Biermann, H. W. *Rev. Chem. Intermed.* **1994**, *20*, 423−445.
(26) Finlayson-Pitts, B. J.; Pitts, J. N. *Chemistry of the Upper and Lower Atmosphere: Theory, Experiments and Applications*; Academic Press: San Diego, 2000; and references therein.
(27) Goodman, A. L.; Underwood, G. M.; Grassian, V. H. *J. Phys. Chem. A.* **1999**, *103*, 7217−7223.
(28) Barney, W. S.; Finlayson-Pitts, B. J. *J. Phys. Chem. A* **2000**, *104*, 171−175.
(29) Sjodin, A.; Ferm, M. *Atmos. Environ.* **1985**, *19*, 985−992.
(30) Notholt, J.; Hjorth, J.; Raes, F. *Atmos. Environ.* **1992**, *26A*, 211−217.
(31) Calvert, J. G.; Yarwood, G.; Dunker, A. M. *Res. Chem. Intermed.* **1994**, *20*, 463−502.
(32) Atkinson, R. *Atmos. Environ.* **1986**, *20*, 408−409.
(33) Wayne, L. G.; Yost, D. M. *J. Chem. Phys.* **1951**, *19*, 41−47.
(34) Graham, R. F.; Tyler, B. J. *J. Chem. Soc., Faraday Trans. 1* **1972**, *68*, 683−688.
(35) Chan, W. H.; Nordstrom, R. J.; Calvert, J. G.; Shaw, J. H. *Chem. Phys. Lett.* **1976a**, *37*, 441−446.
(36) Chan, W. H.; Nordstrom, R. J.; Calvert, J. G.; Shaw, J. H. *Environ. Sci. Technol.* **1976b**, *10*, 674−682.
(37) Kaiser, E. W.; Wu, C. H. *J. Phys. Chem.* **1977b**, *81*, 1701−1706.
(38) Sakamaki, F.; Hatakeyama, S.; Akimoto, H. *Int. J. Chem. Kinet.* **1983**, *15*, 1013−1029.
(39) Pitts, J. N.; Sanhueza, E.; Atkinson, R.; Carter, W. P. L.; Winer, A. M.; Harris, G. W.; Plum, C. N. *Int. J. Chem. Kinet.* **1984a**, *16*, 919−939.
(40) Bartram, M. E.; Koel, B. E. *Surf. Sci.* **1989**, *213*, 137−156.
(41) Wang, J.; Koel, B. E. *J. Phys. Chem.* **1998**, *102*, 8573−8579.

(42) Sato, S.; Yamaguchi, D.; Senga, T.; Kawasaki, M. *J. Phys. Chem. B* **2000**, *104*, 4863.

(43) Kiselev, A. V.; Lygin, V. I. *Infrared Spectra of Surface Compounds*; Wiley: New York, 1975.

(44) Elmer, T. H. Porous and Reconstructed Glasses. In *Engineered Materials Handbook*; ASM International: Materials Park, OH, 1992; Vol. 4, Ceramic and Glasses, pp 427−432.

(45) Mochida, M.; Finlayson-Pitts, B. J. *J. Phys. Chem. A.*, submitted for publication.

(46) Devi, V. M.; Fridovich, B.; Jones, G. D.; Snyder, D. G. S. *J. Mol. Spectrosc.* **1982**, *93*, 179−195.

(47) Valyon, J.; Hall, W. K. *J. Phys. Chem.* **1993**, *97*, 1204−1212.

(48) Chao, C. C.; Lunsford, J. H. *J. Am. Chem. Soc.* **1971**, 6794−6800.

(49) DeMore, W. B.; Sander, S. P.; Golden., D. M.; Hampson, R. F.; Kurylo, M. J.; Howard, C. J.; Ravishankara, A. R.; Kolb, C. E.; Molina, M. J. Chemical Kinetics and Photochemical Data for Use in Stratospheric Modeling, Evaluation No. 12. In *JPL Publ.* 1997; Vol. No. 97-4.

(50) Grätzel, M.; Taniguchi, S.; Henglein, A. *Ber. Bunsen-Ges. Physik. Chem.* **1970**, *74*.